RESEARCH ARTICLE

Brucea javanica (L.) Merr Seed Extract Exerts Antihypertensive and Renoprotective Activity in Renovascular Hypertensive Mice Model

Candra Dwipayana Hamdin[1,*], Mursal Ghazali[2], Pantawane Amit Ravindra[3], Reymund Callanga Derilo[4], Vania Aisyah Aulia Syahda Haris[1], Windi Andika[1], Lalu Rudyat Telly Savalas[5]

[1]Study Program of Pharmacy, Faculty of Medicine and Health Science, University of Mataram, Jl. Majapahit No. 62, Mataram, Indonesia
[2]Department of Biology, Faculty of Mathematics and Natural Sciences, University of Mataram, Jl. Majapahit No. 62, Mataram, Indonesia
[3]National Tsing Hua University, No. 101, Section 2, Kuang-Fu Road, Hsinchu City, Taiwan
[4]Nueva Vizcaya State University - Bambang Campus, Heroes Boulevard, Bambang 3702, Nueva Vizcaya, Philippines
[5]Study Program of Chemistry Education, Faculty of Teacher Training and Education, University of Mataram, Jl. Majapahit No. 62, Mataram, Indonesia

*Corresponding author. Email: candradwipayana@unram.ac.id

Received date: Sep 24, 2026; Revised date: Oct 21, 2026; Accepted date: Oct 23, 2026

Abstract

BACKGROUND: Renovascular hypertension (RVH) drives excessive renin-angiotensin-aldosterone system (RAAS) activation, oxidative stress, and vascular remodelling, but most of current RVH therapies may not fully prevent the disease progression. *Brucea javanica* seed is known to contain bioactive compound that modulate RAAS and regulate blood pressure, but their effects on RVH remain unclear. This study was conducted to evaluate the potential of *B. javanica* seed extract (BJSE) as antihypertensive and renoprotective effects.

METHODS: BJSE were profiled using liquid chromatography–high resolution mass spectrometry (LC-HRMS) and antioxidant activity was assessed. Network pharmacology and molecular docking were conducted to identify compound–protein targets. Male BALB/c mice was RVH-induced by renal blood flow restriction surgery and received either: no treatment, captopril, or, 10, 20, 30 mg/kg BW BJSE. Healthy mice were also included as control. Blood pressure, urinalysis, haematology, renal function, gross pathology, and kidney-heart histology were evaluated.

RESULTS: Ten major metabolites were identified, including flavonoids, phenolic acids, and terpenoids. Antioxidant assays showed IC_{50} values of 71.81±0.35 ppm (DPPH), 76.30±0.29 ppm (FRAP), and 49.45±0.26 ppm (ABTS). Network pharmacology revealed five hub genes (matrix metallopeptidase 9 (*MMP9*), peroxisome proliferator-activated receptor gamma (*PPARG*), nitric oxide synthase 3 (*NOS3*), angiotensin-converting enzyme (*ACE*), estrogen receptor 1 (*ESR1*)), further molecular docking showed phloretin has the highest potential binding with ACE mapped to RAAS. BJSE dose-dependently reduced systolic blood pressure, proteinuria, blood urea nitrogen (BUN), and creatinine, improved erythrocyte parameters and leukocyte counts, and attenuated renal atrophy, cardiac hypertrophy, and histopathological lesions.

CONCLUSION: BJSE significantly reduced blood pressure and improved cardiac and renal histopathological profiles, as well as hematological and urinary parameters associated with renoprotective activity. These effects are achieved suggested due to its antioxidant activity and multi-targeted mechanisms.

KEYWORDS: polycystic ovary syndrome, *Brucea javanica*, network pharmacology, renin-angiotensin-aldosterone system, renovascular hypertension, two-kidney-one-clip

Indones Biomed J. 2026; 18(5): 498-512

Copyright © 2026 The Prodia Education and Research Institute.
This work is licensed under a Creative Commons Attribution-NonCommercial 4.0 International (CC-BY-NC) License.

Introduction

Hypertension remains one of the leading contributors to cardiovascular morbidity and mortality worldwide, affecting more than 1.13 billion individuals. Despite advances in antihypertensive therapy, optimal blood pressure control remains challenging, particularly in secondary hypertension.(1) Among the secondary causes of hypertension, renovascular hypertension (RVH) is primarily caused by renal artery stenosis, resulting in reduced renal perfusion and persistent activation of renin–angiotensin–aldosterone system (RAAS). Excessive RAAS activation promotes vasoconstriction, sodium and water retention, oxidative stress, endothelial dysfunction, and vascular remodelling, accelerating hypertension and increasing the risk of cardiovascular and renal complications. Consequently, RAAS is an important therapeutic target in RVH.(2) Current therapeutic strategies for RVH include pharmacological treatment with angiotensin-converting enzyme inhibitors (ACEi), angiotensin II receptor blockers (ARBs), and calcium channel blockers (CCB).(3) However, current therapies may not fully prevent disease progression and may cause renal artery failure, highlighting the need for alternative agents targeting RAAS dysregulation, oxidative stress, and vascular dysfunction.(4)

Brucea javanica (L.) Merr. is a traditional medicine plant that contains bioactive secondary metabolites, including flavonoids, terpenoids, and phenolic compounds. Ethnopharmacological reports from Indonesia and the Indo-Malay region document the use of *B. javanica* seeds for managing blood pressure.(5) Furthermore, previous studies have found that *B. javanica* seed extract (BJSE) possesses antioxidant, nephroprotective, and vasoprotective activities through modulation of oxidative stress, inflammatory mediators, and intracellular signalling pathways.(6) Previous study on phytochemical analyses of BJSE have identified compounds such as phloretin, chlorogenic acid, and other phenolic acids, some of which have demonstrated potential ACE-inhibitory activity *in vitro*.(7,8) These findings provide a rationale for investigating BJSE as a potential therapeutic candidate for RVH.

Despite the pharmacological activities of *B. javanica* that have been extensively reported, its therapeutic potential against RVH remains insufficiently studied. Therefore, in this study, liquid chromatography–high resolution mass spectrometry (LC-HRMS) metabolite profiling, *in silico* prediction of molecular interaction, as well as *in vitro* and *in vivo* evaluation were integrated to investigate the potential anti-renovascular hypertension effect of BJSE.

Methods

Characteristics of *B. javanica* Extract and Bioactive Compound Identification

B. javanica seeds were collected from Sesaot, Narmada District, West Lombok, Indonesia. *B. javanica* seeds were dried at 24°C, ground, and extracted using ultrasonic-assisted extraction (UAE) with 96% ethanol for 3×15 minutes at 30°C, then evaporated at 40°C.(9) For metabolite profiling using LC-HRMS, the extract was dissolved in methanol, sonicated for 15 minutes, centrifuged at 10,000 rpm for 10 minutes, and filtered (0.22 µm). C18 column separation used a water (A) and methanol (B) (both 0.1% formic acid), from 100% A to 95% B (1.5-18.5 minutes), and held for 10 minutes at 0.3 mL/min. Full-scan mass spectrometry (MS1) was acquired at m/z 100–1000 (240,000 resolution), followed by tandem mass spectrometry (MS/MS) at 30,000 resolution. Mass accuracy (<2 ppm) was ensured by EASY-IC™, with AcquireX (Thermo Fisher Scientific, Waltham, MA, USA). Analyses were performed in triplicate with blank and pooled controls.

In vitro Antioxidant Assays

Antioxidant activity was evaluated via 2,2-diphenyl-1-picrylhydrazyl (DPPH), (2,2′-azino-bis(3-ethylbenzothiazoline-6-sulfonic acid) (ABTS), and ferric reducing antioxidant power (FRAP) assay using vitamin C or gallic acid as standard (Sigma-Aldrich, St. Louis, MO, USA). For DPPH, 100 µL of serially diluted extract or standard was mixed with 100 µL of DPPH, incubated at 37°C for 30 minutes, and measured at 517 nm. For FRAP, 20 µL sample was added to 280 µL of FRAP reagent and read at 492 nm. For ABTS, 10 µL sample was mixed with 290 µL of ABTS solution and measured at 630 nm.(10)

Network Pharmacology Analysis

Bioactive compounds from *B. javanica* seeds LC-HRMS profiling were identified via literature review, with Canonical SMILES retrieved from PubChem. Compound targets were predicted using SwissTargetPrediction, while renovascular hypertension-related targets (arterial stenosis, vascular remodelling) were collected from GeneCards. Intersections targets were considered potential therapeutic targets. A compound-targets-disease network was constructed in Cytospace v3.10.4. Intersections targets were imported into STRING (Homo sapiens, confidence ≥0.900) to build a protein-protein interaction (PPI) network, exported to Cytoscape for topological analysis, and hub genes were identified via CytoHubba. Functional enrichment

was performed using ShinyGO v0.81 (p<0.05), false discovery rate (FDR) <0.05 with Database for Annotation, Visualization and Integrated Discovery (DAVID) validation. Genes enriched in dominant terms and identified as PPI hub genes were prioritized for molecular docking and dynamics simulations.

Molecular Docking of *B. javanica* Constituents Against Hub Targets

Molecular docking was performed using AutoDock Tools version 1.5.7 and AutoDock 4.2.6. Docking simulations employed the Lamarckian Genetic Algorithm (LGA) with 100 runs per ligand. Results were evaluated based on binding energy, root mean square deviation (RMSD), and ligand–protein interactions. The protein targets and candidate compounds selected for molecular docking were determined based on the network pharmacology analysis.

***In vivo* Experimental Procedure and Renovascular Hypertension Modelling**

Thirty-six male BALB/c mice were randomly divided into six groups: healthy mice as normal control, untreated RVH-induced mice as negative control, RVH-induced mice received 25 mg/kg BW captopril as positive control, and RVH-induced receiving either 10, 20, and 30 mg/kg BW BJSE (BJ10, BJ20, and BJ30) as treatment groups. After 7 days of acclimatization, RVH was induced on day-8 by renal blood flow restriction surgery. Mice were anesthetized with ketamine-midazolam (1.5:1), and the left renal artery was exposed through a dorsalis sinistra incision and constricted with a 0.2 mm clip for 15 minutes, after which clip was removed; the right kidney remained untouched. Incisions were closed and recovery was monitored before single housing with free access to feed and water. Mice with severe post-operative stress and infection at the incision site, or had died were excluded from the study.

Treatments commenced 24 hours post-surgery and were administered once daily for 14 days by oral gavage. Food intake and water intake were recorded daily, while body weight was measured every 3 days. Urine was collected on day-24. On day-25, systolic blood pressure (SBP) and blood samples were collected. Subsequently, kidney and heart were isolated for gross pathology and histology (Supplementary 1).

Biological Samples Collection

Urine was collected over 24 hours using a metabolic cage. Samples were immediately transferred into sterile tubes and identified using a urine dipstick test. Blood was collected after an 8-hour fast via intracardiac puncture. Mice were placed in dorsal decubitus and a 27G×8 mm needle was inserted. A 300 µL aliquot was collected into an EDTA-K2 tube, mixed in a homogenizer, and analysis using an automated hematology analyzer.

Blood Pressure Evaluation

Blood pressure was evaluated invasively through left ventricle on day-14 post-treatment. An intrathoracic incision was made through anterior thoracic wall to expose lungs and cardiac silhouette. A 26G abocath was inserted into left ventricle and pressure was recorded by mercury manometer.

Evaluation of Gross Pathology and Histology of Kidney and Heart

Macroscopic observation of kidney and heart morphology was performed across all groups. Organs were cleaned of adipose tissue and assessed for size, colour, texture, and weight. Data were analysed and compared against the normal group.(11)

The left (stenotic) and right kidneys (contralateral) along with the heart were isolated, washed, fixed in 10% formalin for 24 hours, and rinsed for 15 minutes, dehydrated through graded alcohols (30%, 50%, 70%, 95%, and 100%) for 30 minutes each, cleared in xylene, and embedded in paraffin. Blocks were sectioned at 5 µm. Sections were deparaffinized, rehydrated, stained with hematoxylin and eosin (H&E), and observed at 400× magnification.(11)

Statistical Analysis

The data are presented as mean±standard error of the mean (SEM). One-way analysis of variance (ANOVA) followed by Tukey's post-hoc test was used for single-time-point measurements, while two-way ANOVA followed by Tukey's post-hoc test was applied for repeated daily measurements. GraphPad Prism 10.4.1 was used, with significance at p<0.05.

Results

BJSE Contains Bioactive Metabolites with Antioxidant Activity

Dried simplicia obtained of 4 kg and yielded a simplicia percentage of 29.5%. The data show that 1.18 kg of simplicia produced 128 grams of viscous extract (10.85%). LC-HRMS identified ten major secondary metabolites, comprising flavonoids, phenolic acids, and terpenoids (Figure 1A-1C and Supplementary 2). Terpenoids included (-)-borneol

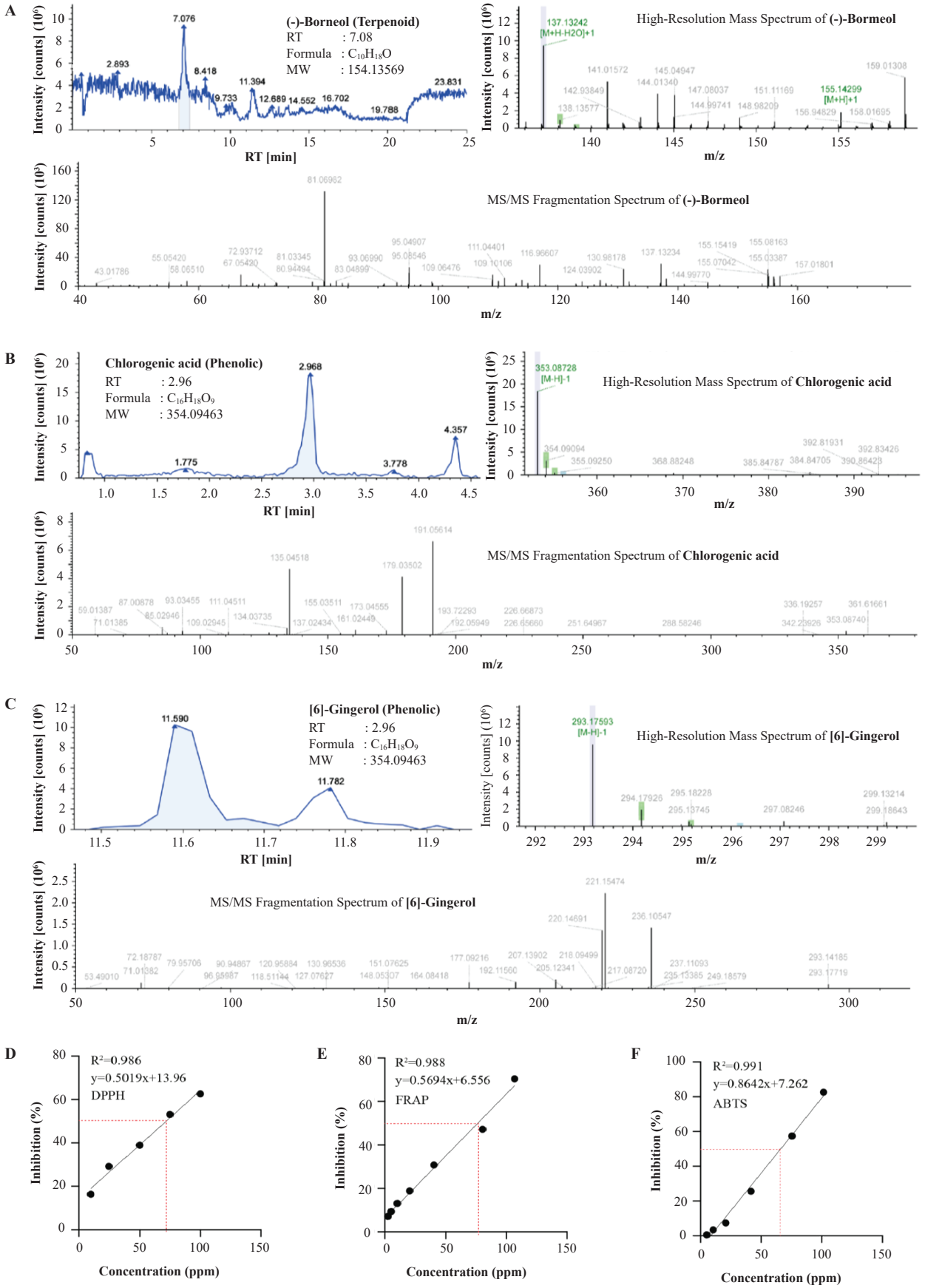


Figure 1. Identification of active constituents and antioxidant evaluation. A–C: LC-HRMS chromatograms, HRMS, and MS/MS spectra identifying (-)-Borneol, Chlorogenic acid, and [6]-Gingerol. D–F: Multi approaches of antioxidant activity including DPPH, FRAP, and ABTS scavenging activities. R^2 and regression equations are shown in each panel.

(dehydrated adduct, m/z 137) and (S)-abscisic acid (m/z 247). Phenolic acids were chlorogenic acid (m/z 353) and isoferulic acid (m/z 193). The [6]-Gingerol was detected at m/z 293. Flavonoids included diosmetin (m/z 301), chrysin (m/z 566), protofarrerol (m/z 319), phloretin (m/z 275), and icariin (m/z 677). Antioxidant activity showed DPPH IC_{50} of 71.81±0.35 ppm; FRAP RP_{50} of 76.30±0.29 ppm; and ABTS IC_{50} of 49.45±0.26 ppm (Figure 1D-1F, Supplementary 3).

ACE Emerges as the Central RAAS-Linked Hub Gene in Network Pharmacology Analysis

Based on LC-HRMS profiling, ten bioactive compounds were screened for potential involvement in RVH (Figure 2). From this analysis, computational identification yielded 11 intersected target genes from cross-mapping between 157 *B. javanica* compounds targets and 89 RVH-associated genes (Figure 2A). A PPI network was constructed with a confidence score threshold of 0.7 and network topology analysis identified five hub genes, namely matrix metallopeptidase 9 (*MMP9*), peroxisome proliferator-activated receptor gamma (*PPARG*), nitric oxide synthase 3 (*NOS3*), angiotensin-converting enzyme (*ACE*), estrogen receptor 1 (*ESR1*) (Figure 2B).

Network visualization revealed a multi-component interaction pattern, in which six principal bioactive constituents, such as Chlorogenic acid, Isoferulic acid, Phloretin, (-)-Borneol, (S)-Abscisic acid, and [6]-Gingerol, interacted with the five hub genes. Based on the biological process category (Figure 2C), enrichment analysis identified cellular response to lipid, regulation of inflammatory response, and blood vessel morphogenesis as the most predominant biological processes. In molecular function (Figure 2D), the highest fold enrichment values were obtained for nuclear estrogen receptor activity and estrogen response element binding. Kyoto Encyclopedia of Genes and Genomes (KEGG) analysis identified 20 significant signaling pathways (Figure 2E). Path view mapping on RAAS pathway confirmed ACE as the only hub gene mapped onto this pathway (Figure 2F).

Molecular Docking Predicts Favorable Binding of *B. javanica* Constituents to *ACE*, *PPARG*, *MMP-9*, *ESR1*, and *eNOS*

Molecular docking validation was performed by redocking the native ligands lisinopril (*ACE*), rosiglitazone (*PPARG*), ARP-100 (*MMP9*), clomifene (*ESR1*), and 6-nitroindazole (*eNOS*) (Supplementary 4), yielding RMSD values of 1.301, 0.911, 1.079, 0.813, and 1.070 Å, respectively (Figure 2G), with all RMSD values were below 2.0 Å. Phloretin bound ACE with an energy of −5.49 kcal/mol, compared with −8.49 kcal/mol for lisinopril. Notably, Phloretin interacted with Glu384, His353, Lys511, and His513, the same residues engaged by lisinopril. For *PPARG*, 6-gingerol showed a binding energy of −6.27 kcal/mol and formed hydrogen bonds with Ser289, His323, Tyr473, and Cys285. Tyr473 is located on helix H12, whereas Cys285 is located on H3. Against *MMP-9*, phloretin, isoferulic acid, and chlorogenic acid gave binding energies of −5.55, −5.15, and −6.26 kcal/mol, respectively. Phloretin and chlorogenic acid formed hydrogen bonds with Leu88. For *ESR1*, phloretin, borneol, isoferulic acid, and abscisic acid yielded −7.94, −5.79, −4.52, and −6.95 kcal/mol. Phloretin hydrogen-bonded with Glu353 and Leu346, borneol and abscisic acid with Glu353, while isoferulic acid showed no interactions with identified residues.

BJSE Reduces Systolic Blood Pressure and Maintains Physiological Parameters

Water intake differed markedly across groups (Figure 3A). Negative control showed highest consumption (25.0–26.0 mL/mice), nearly double normal controls (14.0–15.0 mL/mice). BJSE treatment reduced water intake dose-dependently, such as 10 mg/kg BW BJSE (23.0–24.0 mL/mice), 20 mg/kg BW BJSE (21.0–22.0 mL/mice), and 30 mg/kg BW BJSE (20.0–21.0 mL/mice). Feed consumption was consistent across all groups (Figure 3B), though negative control experienced a transient drop during the first few days post-surgery but recovered by day 7. Body weight remained stable over 14-day (p>0.05). Captopril recorded the highest mean weight (23.77±0.50 g), while hypertensive control showed the lowest (21.93±0.84 g) (Figure 3C). SBP showed that normal and positive groups had the lowest SBP (125 and 127 mmHg, respectively), while negative group showed the highest SBP (158 mmHg). BJSE at 10, 20, and 30 mg/kg reduced SBP dose-dependently to approximately 150, 138, and 130 mmHg, respectively. The SBP results correlated positively with water intake data (Figure 3D).

Dose-Dependent Improvement in Urinary, Hematological, and Renal Function Markers

Urinalysis results showed severe proteinuria in negative control, indicating significant renal impairment compared to control. Captopril produced moderate proteinuria, while BJSE demonstrated dose-dependent reduction (Table 1, Supplementary 5). Hematological analysis revealed markedly reduced erythrocyte parameters, leukocytosis, and elevated platelets in negative control compared to normal (Supplementary 6). Renal function markers were

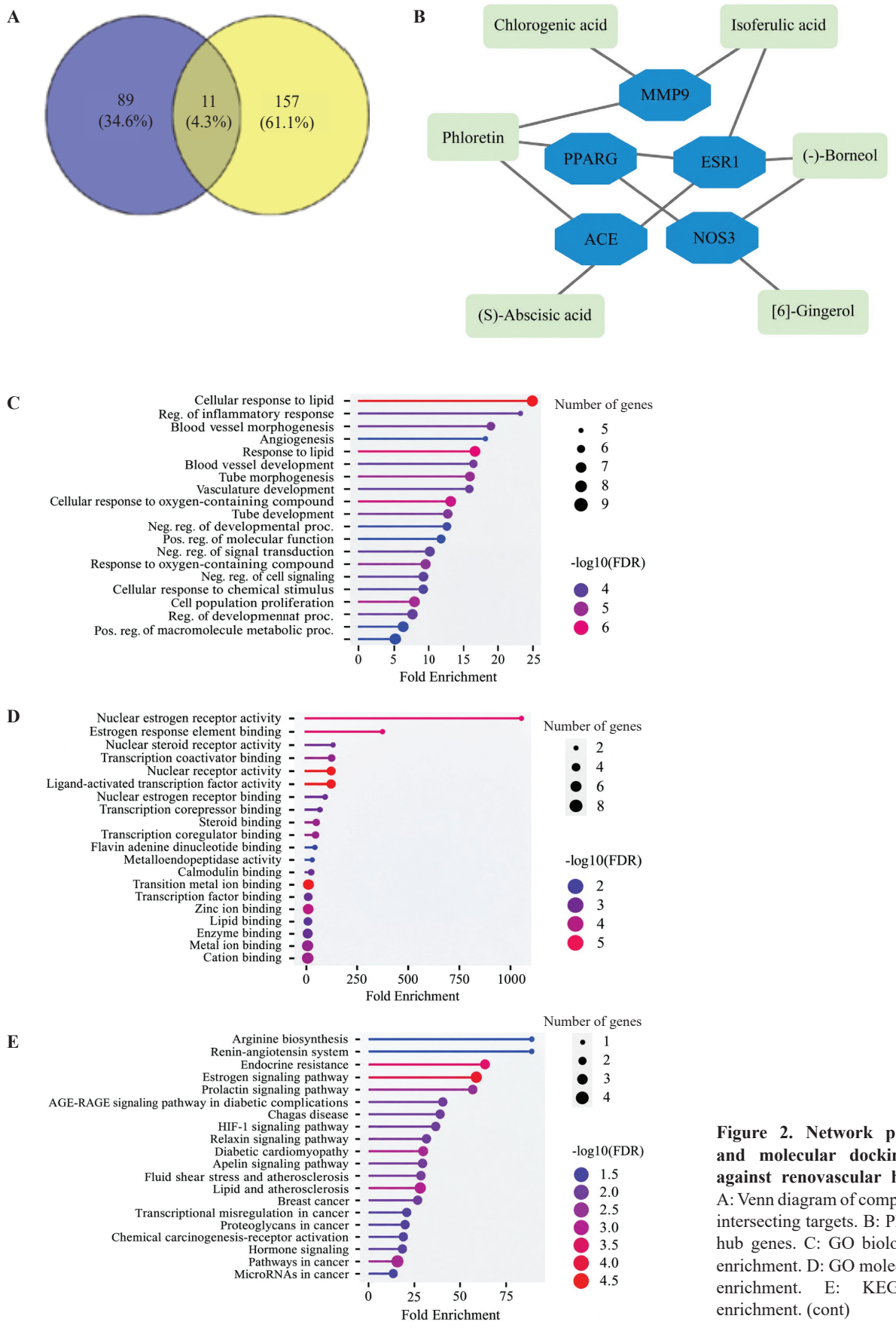
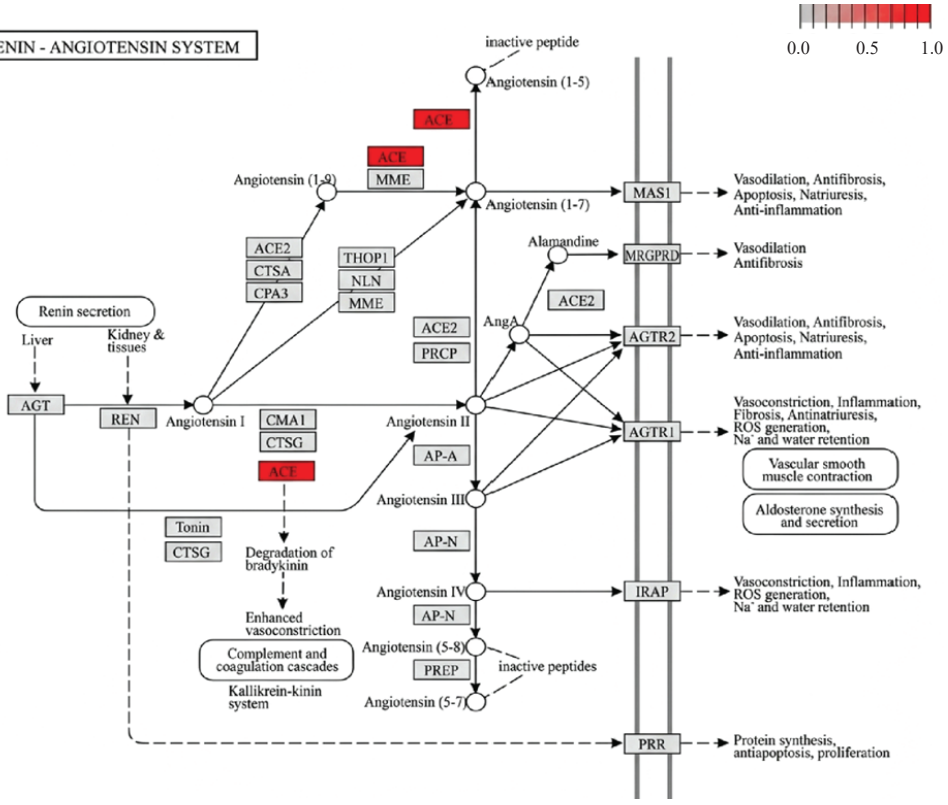
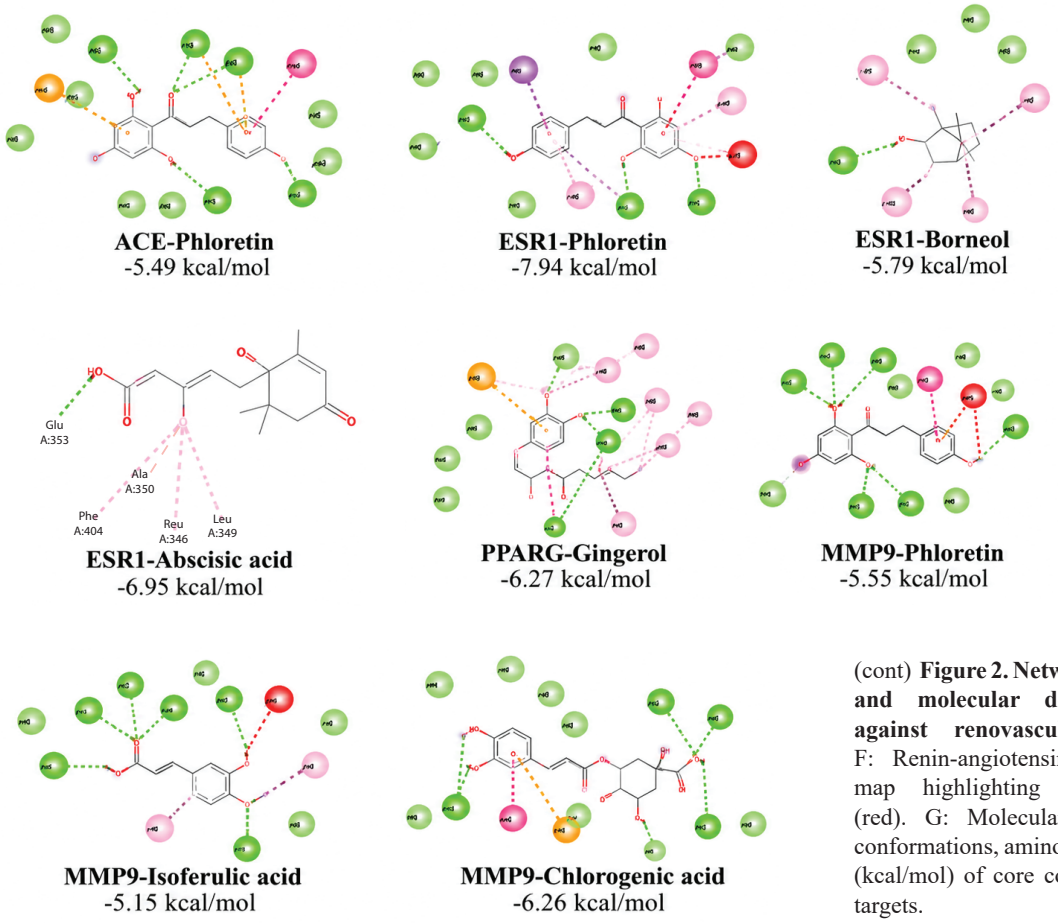


Figure 2. Network pharmacology and molecular docking of BJSE against renovascular hypertension. A: Venn diagram of compound–disease intersecting targets. B: PPI network of hub genes. C: GO biological process enrichment. D: GO molecular function enrichment. E: KEGG pathway enrichment. (cont)

F



G



(cont) **Figure 2. Network pharmacology and molecular docking of BJSE against renovascular hypertension.** F: Renin-angiotensin system pathway map highlighting the ACE target (red). G: Molecular docking binding conformations, amino acids, and affinities (kcal/mol) of core compounds with hub targets.

severely elevated in negative control. Additionally, BJ treatment produced dose-dependent improvements across all parameters, with 30 mg/kg BW BJSE group showing the most favorable recovery (Table 1).

BJSE Preserves Renal and Cardiac Morphology

Negative control exhibited stenotic kidney atrophy with surface irregularities and contralateral kidney hypertrophy (Figure 4A). Captopril partially preserved stenotic kidney morphology with less pronounced atrophy. Kidney length measurements followed a similar pattern, with negative control showing contralateral lengthening (1.12 cm *vs.* normal 0.95 cm) and stenotic shortening (0.71 cm). The 30 mg/kg BW BJSE group had restored lengths to near normal (0.98 cm, 0.90 cm), comparable to captopril (Figure 4A). Kidney weight ratio analysis showed that the stenotic

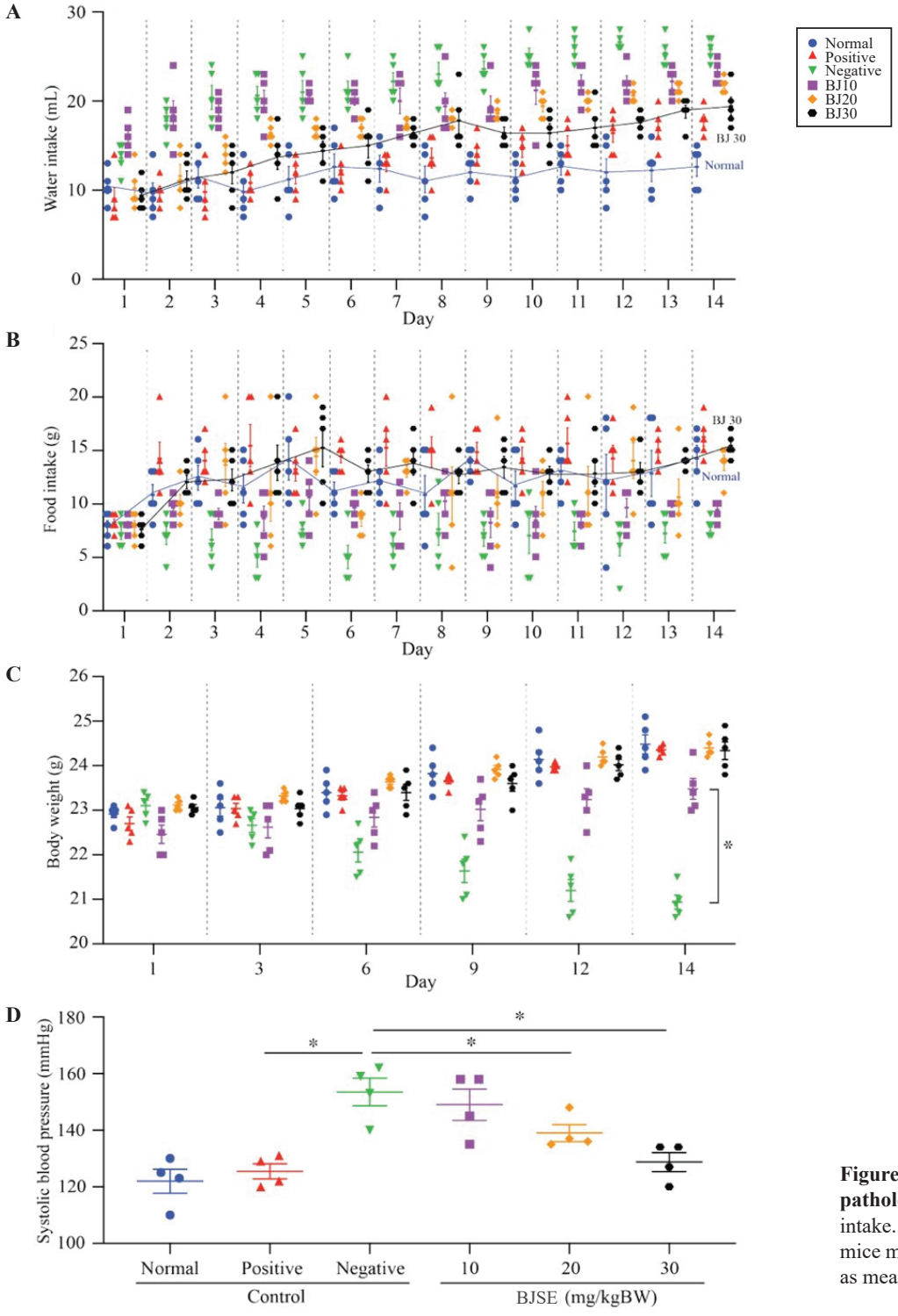


Figure 3. Effect of BJSE on clinical pathology. A: Water intake. B: Food intake. C: Body weight. D: SBP in mice model over 14 days. Data shown as mean±SEM (n = 4-5).

Table 1. Urinalysis and haematology profile from all experimentals groups.

Parameters	Groups					
	Normal	Positive	Negative	BJ10	BJ20	BJ30
Urine						
Proteinuria	-	++	++++	+++	+	+
pH	5	8	8.5	8.5	8	8
Haematuria	-	-	-	-	-	-
Specific gravity	1.02	1.03	1.00	1.01	1.02	1.03
Hematology						
RBC (10^6/µL)	8.803±0.188	8.025±0.053	5.143±0.357	6.233±0.181	7.740±0.314	7.858±0.336
HB (g/dL)	11.85±0210	10.18±0.375	7.00±0.414	7.50±0.500	9.65±0.523	10.28±0.295
HCT (%)	39.57±0.482	38.35±0.688	27.67±0.729	31.37±0.495	34.55±0.703	36.20±0.430
Leukocyte (10^3/µL)	5.89±0.228	6.24±0.427	10.72±0.125	9.08±0.343	7.99±0.455	7.31±0.190
Lymphocyte	79.55±0.504	79.55±0.504	67.90±0.598	72.15±0.829	74.87±0.715	77.35±0.464
Monocyte (%)	2.77±0.239	3.50±0.191	6.80±0.108	5.55±0.246	4.45±0.246	4.07±0.165
Neutrophil (%)	19.45±0.783	21.70±0.819	28.40±1.00	25.42±0.913	23.77±0.618	22.30±0.527
Thrombocyte (10^3/µL)	1022±32.17	1057±34.01	1354±24.01	1301±29.27	195±13.84	1048±48.17
BUN (mg/dL)	15.02	17.6	34.67	32.2	25.67	21.45
Creatinin (mg/dL)	0.23	0.33	0.9	0.78	0.54	0.4

kidney negative control had a reduced ratio (93×10^{-4} g), while contralateral kidney (84×10^{-4} g) compared to normal (83.6×10^{-4} g). BJSE treatment normalized these ratios dose-dependently; 30 mg/kg BW BJSE stenotic (85.4×10^{-4} g) and contralateral (78×10^{-4} g) approached captopril values (83.8×10^{-4} g and 74×10^{-4} g) (Figure 4B).

Cardiac examination revealed hypertrophy in negative control characterized by enlarged heart and thickened ventricular walls (Figure 4C). Captopril significantly improved cardiac morphology. Heart length followed similar trends that negative (0.93 cm) *vs.* normal (0.838 cm); 30 mg/kg BW BJSE (0.778 cm) and captopril (0.834 cm) approached normal values (Figure 4C). The heart weight-to-body weight ratio was elevated in negative control (61.80×10^{-4} g) compared to normal (48.75×10^{-4} g). BJSE treatment showed dose-dependent reduction, comparable to captopril 49.43×10^{-4} g (Figure 4D).

BJSE Attenuates Histopathological Lesions in Heart and Kidney

Negative control group showed extensive vacuolar degeneration in cardiomyocytes (black arrows) (Figure 5A), with the score of 2.22±0.28 vs. normal ($p<0.001$). Captopril reduced the score (0.46±0.35), while BJSE treatment showed dose-dependent improvement (Figure 5D). The stenotic kidney in negative control exhibited marked vacuolar degeneration with inflammatory cell infiltration (Figure 5B), while contralateral kidney showed similar but less severe changes (Figure 5C). Contralateral kidney quantification confirmed negative control had the highest score, (3.2±0.20), with BJ10 (2.25±0.18), BS20 (1.96±0.19), and BJ30 (0.55±0.24) showing dose-dependent improvement comparable to positive (1.52±0.28).

Evaluation of stenotic kidney encompassed six histopathological parameters (Figure 5F). Negative control exhibited the highest scores across all parameters; epithelial degeneration (3.1±0.26), epithelial necrosis (3.0±0.67), glomerular necrosis (3.15±0.34), glomerular infiltration (2.88±0.25), glomerular sclerosis (2.87±0.27), and interstitial fibrosis (2.12±0.84). Captopril significantly reduced all parameters to scores ranging from 1.0 to 1.47. BJSE demonstrated dose-dependent improvement, with 30 mg/kg BW BJSE showing the most favourable recovery; epithelial degeneration (0.88±0.30), epithelial necrosis (1.45±0.47), glomerular necrosis (0.50±0.50), glomerular infiltration (1.12±0.30), glomerular sclerosis (0.34±0.20), and interstitial fibrosis (1.02±0.25), approaching captopril values across all parameters.

Discussion

The yield of BJSE (10.85%) was consistent with previous reports, with variations likely due to differences in plant

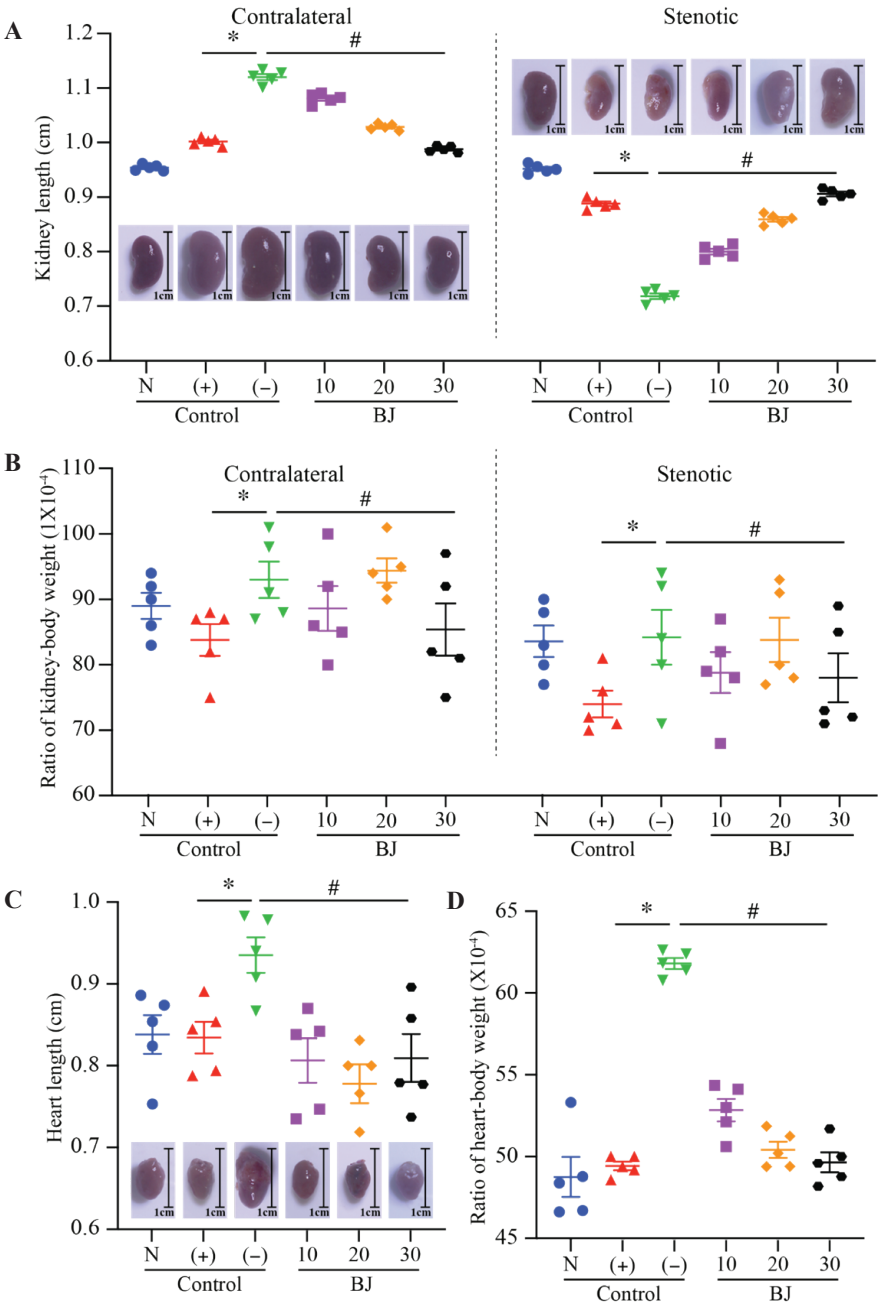


Figure 4. Effect of BJSE treatment on renal and cardiac morphology in renovascular hypertensive mice. A: Kidney length. B: Kidney-to-body weight ratio. C: Heart length. D: Heart-to-body weight ratio. Data are presented as mean±SEM (n=5 per group). Panels A, B, C, and D were analyzed using one-way ANOVA followed by Tukey's multiple comparison test; *$p<0.05$, $^{\#}p<0.05$ *vs.* negative control.

material, extraction methods, solvent, and geographic location.(12) The LC-HRMS analysis revealed the presence of a variety of secondary metabolites which include flavonoids, phenolic acids, and terpenoids compounds (Figure 1A-C). Many of metabolites influence vascular function including diosmetin, icariin, and chrysin which effect ACE and AT1R signaling (13); cholorogenic acid on ACE inhibition; isoferulic acid and (S)-abscisic acid on eNOS and NO activity (14); borneol, [6]-gingerol, and phloretin on vasodilation and oxidative pathways (15).

The extract demonstrated concentration-dependent antioxidant activity in DPPH, FRAP, and ABTS assay that correlated to phenolic and flavonoid content of extract (Figure 1D-1F). BJSE showed DPPH activity that corresponded to the reported literature values (64.703 ppm), with differences potentially attributable to extraction technique, solvent, and phytochemical composition.(10) These findings support the potential contribution of antioxidant activity to the cardiovascular effects of BJSE in RVH.(16)

Network pharmacology identified that *MMP9*, *PPARG*, *NOS3*, *ACE*, and *ESR1* as hub genes suggests that BJ's functions may include vascular remodeling, endothelial, inflammation, and blood pressure control pathways.(17) *ACE* was the only hub gene that was linked to RAAS,

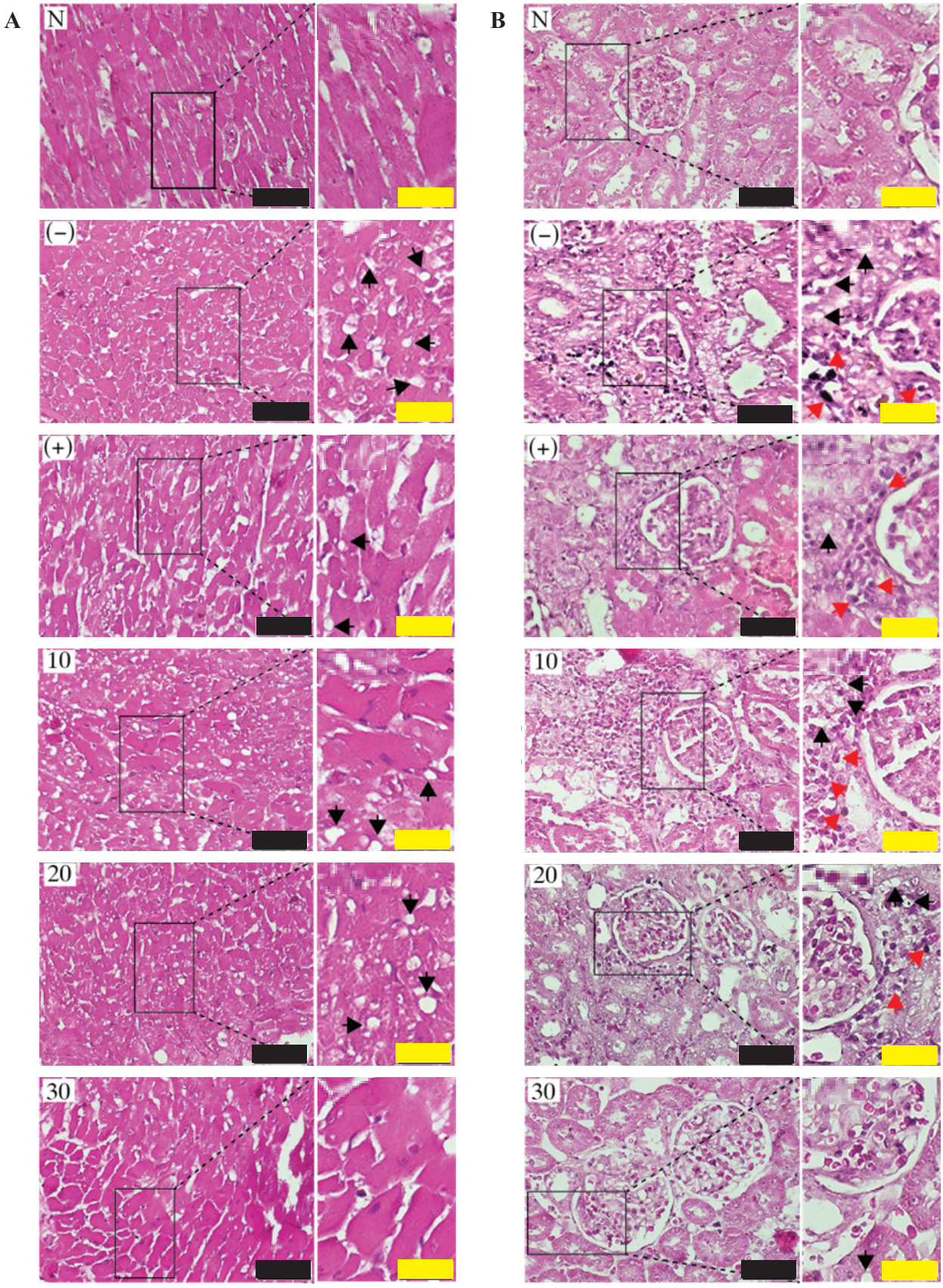
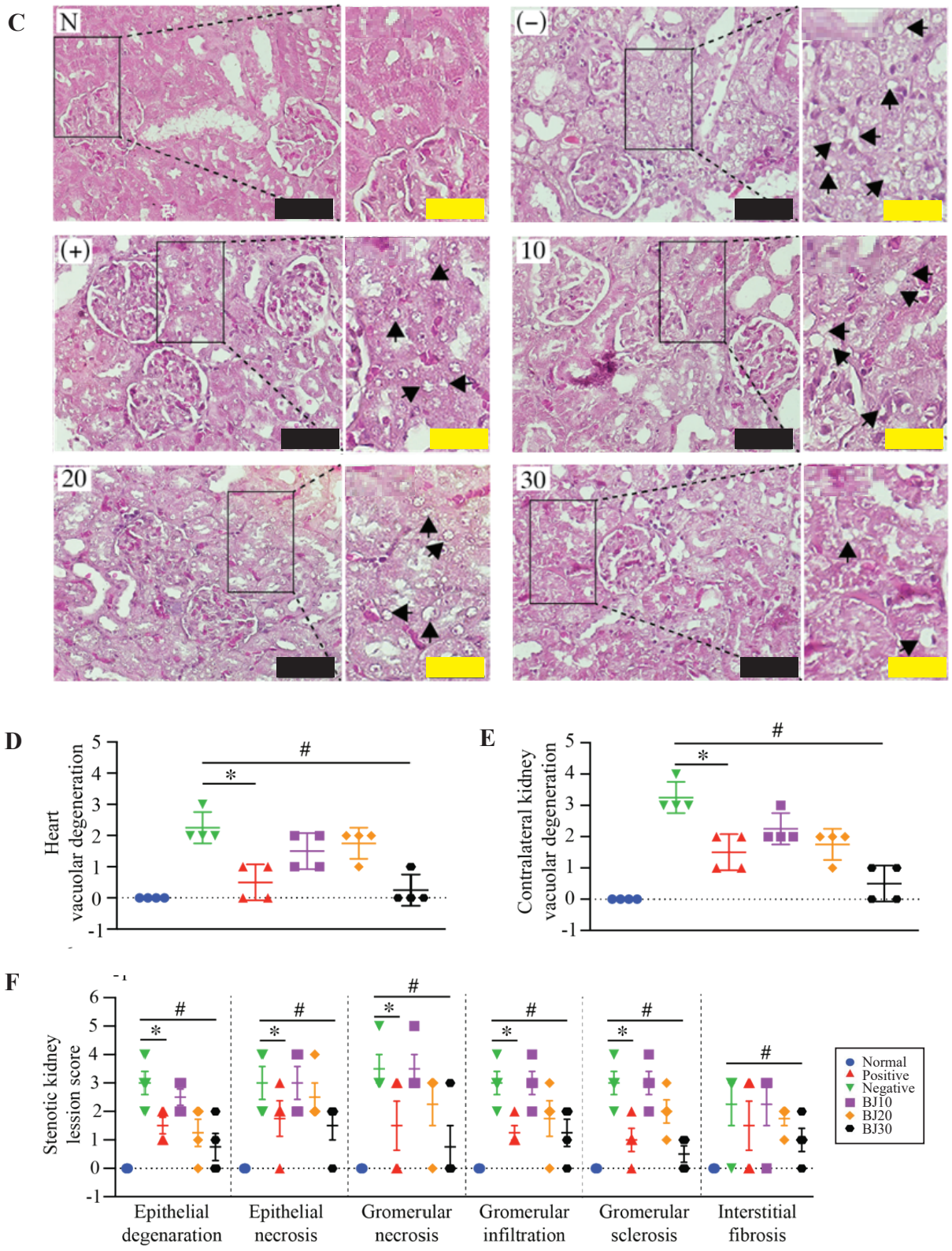


Figure 5. Histopathological evaluation of heart and kidney tissues in renovascular hypertensive mice treated with BJSE. A: Heart histology. B: Stenotic kidney histology. Grouping is as follow: (N): Normal control; (-): Negative control; (+): Positive control; (10): 10 mg/kg BW BJSE; (20): 20 mg/kgBW BJSE; (30): 30 mg/kgBW BJSE. Black arrows indicate vacuolar degeneration; red arrows indicate inflammatory cell infiltration. Black bar: 25 µm; Yellow bar: 100 µm. (cont)



(cont) **Figure 5. Histopathological evaluation of heart and kidney tissues in renovascular hypertensive mice treated with BJSE.** C: Contralateral kidney histology. Grouping is as follow: (N): Normal control; (-): Negative control; (+): Positive control; (10): 10 mg/kg BW BJSE; (20): 20 mg/kgBW BJSE; (30): 30 mg/kgBW BJSE. Black arrows indicate vacuolar degeneration. Black bar: 25 µm; Yellow bar: 100 µm. D: Cardiac vacuolar degeneration score. E: Contralateral kidney vacuolar degeneration score. F: Stenotic kidney histopathological scores. Data are presented as mean±SEM (n=6 per group). *p<0.05 *vs.* normal control, #p<0.05 vs. negative control.

supporting its potential relevance to the antihypertensive effects of BJSE.(2) This finding is consistent with reports of ACE-inhibitory activity associated with chlorogenic acid and other polyphenols.(18) Molecular docking further supported these predictions. Phloretin interacted with Glu384 in the S1 pocket and formed hydrogen bonds with His353, Lys511, and His513 in the S2 pocket of the active site that also engaged by lisinopril (Figure 2G), suggesting that phloretin may bind within the ACE catalytic region and interfere with substrate binding.(19–21) Phloretin and chlorogenic acid bound near the S1' pocket of *MMP-9*, close to the catalytic zinc cite, while phloretin, borneol, and abscidic acid anchored to Glu353 within the *ESR1* ligand-binding domain.(22)

BJSE treatment in RVH mice model exhibited no major systemic intolerance, with minimal changes in body weight and feed consumption, consistent with stability in body weight despite elevated blood pressure in many hypertensive models (Figure 3). The fluctuation in feed intake was likely a stress response since feeding returned to normal.(23) The antihypertensive effect of BJSE is more evident from the reduction in SBP seen at 10–30 mg/kg of BJSE-treated mice (Figure 3D), with network analysis supporting the involvement of ACE, eNOS, and remaining vascular regulatory pathways, consistent with reports that plant-derived antihypertensive compounds regulate blood pressure through complementary mechanisms of vascular tone, oxidative stress, and renal control.(24)

Hypertensive controls exhibited proteinuria, indicating glomerular injury potentially associated with elevated intraglomerular pressure and angiotensin II activity in RVH. (25) BJSE treatment progressively reduced proteinuria (Table 1), particularly at the highest dose, suggesting improved glomerular integrity in association with reduced systolic blood pressure (Figure 3D and 5). The findings are consistent with studies on other plant-derived compounds in the renal hypertensive model, where reduced blood pressure correlated with decreased urinary protein excretion.(26)

Treatment with BJSE improved all parameters haematology in a dose-dependent manner, with 30 mg/kg BW BJSE showing the most pronounced recovery (Table 1). Improvements in erythrocyte indices and reductions in leukocyte counts suggest potential hematopoietic and anti-inflammatory effects, possibly related to antioxidant activities of flavonoids.(27,28) Renal function markers also improved, with BJ30 close to captopril values in line with prior findings on BJ seed extracts in diabetic rats.(7) This improvement may reflect reduced intraglomerular pressure and antioxidant protection of renal tubular cells. (29) Overall, the findings suggest BJSE treatment support a multi-targeted mechanism involving ACEi, eNOS enhancement, and antioxidant activities.(30)

Macroscopic results confirmed the expected effects in RVH model, with atrophy of the stenotic kidney and compensatory hypertrophy of the contralateral kidney. (31) The changes in the control hypertensive group are consistent with chronic renal ischemia (Figure 4), while the progressive improvement in weight and dimension ratios indicates that treatment improved systemic hemodynamic, an interpretation supported by evidence that antihypertensive interventions reduce intraglomerular pressure and limit renal structural remodeling. All control hypertensive mice demonstrated cardiac hypertrophy with higher heart weight-to-body weight ratios, consistent with chronic pressure overload and RAAS activation.(32,33)

BJSE treatment reduced cardiac morphological abnormalities, potentially through decreased hemodynamic stress and antioxidant effects of phenolic compounds.(34) The 30 mg/kg BW BJSE had values that were closer to captopril group, suggesting that BJ may have an important organ-protective effect (Figure 4). Hypertensive controls showed extensive vacuolar degeneration in heart and kidney tissue (Figure 5A-5C), consistent with cellular damage caused by ischemic, oxidative, and hemodynamic injury. (35) Inflammatory infiltration in stenotic kidney further indicated ischemia-associated inflammation, which may contribute to fibrosis and progressive renal dysfunction. (36,37) BJSE treatment at 30 mg/kg significantly reduced the lesions, suggesting that the extract acts at multiple points in this pathological process. This is likely due to the anti-inflammatory and antioxidant activities of diosmetin, icariin, chlorogenic acid, and other *B. javanica* constituents, which may help attenuate oxidative and inflammatory stress and prevent tissue degeneration.(38)

The reduction of inflammatory infiltration and improved contralateral kidney morphology suggest that *B. javanica* may exert systemic effects through modulation of inflammation, circulation, and endothelial function. Together, the improvement in blood pressure, renal function, haematological parameters, and tissue architecture suggest that BJ indicate that BJ may provide multi-targeted protection in RVH through complementary antioxidant, anti-inflammatory, and vascular regulatory mechanisms. Given the limitations of the current study, especially for evaluating the pharmacologic activities of BJ for the treatment of hypertension and renal protection, additional studies are needed. Further studies are necessary to isolate specific active compounds, elucidate precise molecular

mechanisms, and evaluate long-term safety and clinical applicability.

Conclusion

The study demonstrates that BJSE exerts significant anti-renovascular hypertension effects correlated to antioxidant activity. Ten bioactive metabolites were observed, while network pharmacology revealed five hub genes (*MMP9*, *PPARG*, *NOS3*, *ACE*, and *ESR1*) linked to RAAS regulation and vascular remodeling. *In vivo*, BJSE dose-dependently reduced SBP, improved renal function, attenuated proteinuria, and protected renal and cardiac tissue in the RVH model, with 30 mg/kg showing effects comparable to captopril. These findings establish BJSE as a promising natural therapeutic candidate for RVH.

Acknowledgments

The authors would like to express their sincere gratitude to the Institute for Research and Community Service (LPPM) University of Mataram for the research support facilities and the funding with grant number 1719/UN18.L1/PP2026 and drh. Djoko Santoso, as pathologist analyzing the histological profile.

Authors Contribution

CDH conceptualized and designed the research. MG, PAR, and CDH carried out data acquisition and collection. RCD, LRTS, and CDH performed data calculations and analysis. VAASH, WD, and CDH prepared the manuscript draft and designed figures. CDH contributed to the interpretation of results. All authors reviewed and critically revised the manuscript.

Ethical Statement

All experimental procedures were approved by the Animal Experiment Ethics Committee, University of Mataram (015/UN18.F8/ETIK/2026).

Conflict of Interest

The authors have no conflicts of interest to declare.

References

1. McEvoy JW, McCarthy CP, Bruno RM, Brouwers S, Canavan MD, Ceconi C, *et al.* 2024 ESC Guidelines for the management of elevated blood pressure and hypertension. Eur Heart J. 2024 Oct 7; 45(38): 3912–4018.
2. Valentini A, Heilmann RM, Kühne A, Biagini L, De Bellis D, Rossi G. The renin-angiotensin-aldosterone system (RAAS): Beyond cardiovascular regulation. Vet Sci. 2025; 12(8): 777. doi: 10.3390/vetsci12080777.
3. Sarafidis PA, Theodorakopoulou M, Ortiz A, Fernandez-Fernández B, Nistor I, Schmieder R, *et al.* Atherosclerotic renovascular disease: a clinical practice document by the European Renal Best Practice (ERBP) board of the European Renal Association (ERA) and the Working Group Hypertension and the Kidney of the European Society of Hypertension (ESH). Nephrol Dial Transplant. 2023; 38(12): 2835–50.
4. Triantis G, Chalikias GK, Ioannidis E, Dagre A, Tziakas DN. Renal artery revascularization is a controversial treatment strategy for renal artery stenosis: A case series and a brief review of the current literature. Hell J Cardiol. 2022; 65: 42–8.
5. Roswiem AP, Kiranadi B, Bachtiar TSP, Ranasasmita R. Antihypertensive effect of Brucea javanica (L.) (Merr.) fruit extract. Makara J Sci. 2012; 16(2): 71–6.
6. Zhang J, Xu HX, Dou YX, Huang QH, Xian YF, Lin ZX. Major constituents from Brucea javanica and their pharmacological actions. Front Pharmacol. 2022; 13: 853119. doi: 10.3389/fphar.2022.853119.
7. Ablat A, Halabi MF, Mohamad J, Hasnan MHH, Hazni H, Teh S huy, *et al.* Antidiabetic effects of Brucea javanica seeds in type 2 diabetic rats. BMC Complement Altern Med. 2017; 17(1): 94. doi: 10.1186/s12906-017-1610-x.
8. Tedjaningrum RA, Ardhia Cahyani R, Amelia Putri R, Salsabila S, Fitriyanti S, Iqbal Rhamadianto M. Natural ACE-inhibitor candidates for hypertension: A narrative literature review with in silico highlights. Indones J Pharm Educ. 2026; 6(1): 168–89.
9. Meliandari BRD, Hajrin W. The comparison of total phenolic in the extract of wali fruit (Brucea javanica L. Merr) with maceration and sonication extraction cethodes. Ad-dawaa J Pharm Sci. 2022; 5(1): 53–63.
10. Risnadewi WN, Muliasari H, Hamdin CD, Andayani Y. Comparative antioxidant activity of Brucea javanica (L) Merr seed extract derived from maceration and soxhletation method. AIP Conf Proc. 2019; 2199: 060003. doi: 10.1063/1.5141312.
11. Hamdin CD, Wu ML, Chen CM, Ho YC, Jiang WC, Gung PY, *et al.* Dual-specificity phosphatase 6 deficiency attenuates arterial-injury-induced intimal hyperplasia in mice. Int J Mol Sci. 2023; 24(24): 17136. doi:10.3390/ijms242417136.
12. Almira D, Subaidah WA, Ananto AD, Deccati RF, Muliasari H. In vitro concentration optimization of ethanol extract from Makasar fruit seeds (Brucea javanica L. Merr) as an anti-inflammatory agent. J Pijar MIPA. 2021; 16(5): 595–9.
13. Ahmad T, Javed A, Khan T, Althobaiti YS, Ullah A, Almutairi FM, *et al.* Investigation into the antihypertensive effects of diosmetin and its underlying vascular mechanisms using rat model. Pharmaceuticals. 2022; 15(8): 951. doi:10.3390/ph15080951.
14. Serreli G, Le Sayec M, Thou E, Lacour C, Diotallevi C, Dhunna MA, *et al.* Ferulic acid derivatives and avenanthramides modulate endothelial function through maintenance of nitric oxide balance in HUVEC cells. Nutrients. 2021; 13(6): 2026. doi: 10.3390/

nu13062026.

15. Liu Y, Li D, Wang S, Peng Z, Tan Q, He Q, *et al.* 6-gingerol ameliorates hepatic steatosis, inflammation and oxidative stress in high-fat diet-fed mice through activating LKB1/AMPK signaling. Int J Mol Sci. 2023; 24(7): 6285. doi: 10.3390/ijms24076285.
16. Herrmann SM, Textor SC. Current concepts in the treatment of renovascular hypertension. Am J Hypertens. 2018; 31(2): 139–49.
17. Rahayu RF, Prayitno A, Purwanto B, Soewondo W, Nurwati I, Pamungkasari EP, *et al.* Combination of metformin and magnesium citrate reduces TNF-α, NF-κB p65, IL-6, CD4, and MMP-9 expressions in diabetic model rats. Indones Biomed J. 2024; 16(6): 546–52.
18. Wu Z, Li L, Li N, Zhang T, Pu Y, Zhang X, *et al.* Optimization of ultrasonic-assisted extraction of fatty acids in seeds of Brucea javanica (L.) Merr. from different sources and simultaneous analysis using high-performance liquid chromatography with charged aerosol detection. Molecules. 2017; 22(6): 931. doi: 10.3390/molecules22060931.
19. Lu Y, Wang Y, Huang D, Bian Z, Lu P, Fan D, *et al.* Inhibitory mechanism of angiotensin-converting enzyme inhibitory peptides from black tea. J Zhejiang Univ Sci B. 2021; 22(7): 575–89.
20. Tahir RA, Bashir A, Yousaf MN, Ahmed A, Dali Y, Khan S, *et al.* In silico identification of angiotensin-converting enzyme inhibitory peptides from MRJP1. PLoS ONE. 2020; 15(2): e0228265. doi:10.1371/journal.pone.0228265.
21. Zhang Y, Zhao X, Ma X, Li J, Ye X, Wang X, *et al.* Activity analysis and inhibition mechanism of four novel angiotensin I-converting enzyme inhibitory peptides prepared from Flammulina velutipes by enzymatic hydrolysis. Foods. 2025; 14(15): 2619. doi: 10.3390/foods14152619.
22. Lee S, Barron MG. Structure-based understanding of binding affinity and mode of estrogen receptor α agonists and antagonists. PLoS ONE. 2017; 12(1): e0169607. doi:10.1371/journal.pone.0169607.
23. Cata JP, Patiño M, Lacagnina MJ, Li J, Gorur A, Agudelo-Jimenez R, *et al.* A rat model to investigate quality of recovery after abdominal surgery. Pain Rep. 2021; 6(2): e943. doi: 10.1097/PR9.0000000000000943.
24. Sanchez A, Chung SC, Mejia A, Ramirez FE, Shavlik GW, Bivens RL, *et al.* Multiple lifestyle interventions reverses hypertension. Gao Y, editor. Cogent Med. 2019; 6(1): 1636534. doi: 10.1080/2331205X.2019.1636534.
25. Delrue C, Speeckaert MM. Beyond blood pressure: Emerging pathways and precision approaches in hypertension-induced kidney damage. Int J Mol Sci. 2025; 26(15): 7606. doi: 10.3390/ijms26157606.
26. Dong Z, Dai H, Feng Z, Liu W, Gao Y, Liu F, *et al.* Mechanism of herbal medicine on hypertensive nephropathy (Review). Mol Med Rep. 2021; 23(4): 234. doi: 10.3892/mmr.2021.11873.
27. Ozkurt M, Akinci B, Kabadere DeliÖrman S, Özyurt R, Karadağ A, Erkasap N. The effects of quercetin on erythropoietin, hypoxia-inducible factors-1α, 2α, and pyroptosis related genes expression levels in inflammation induced by TNF-α and LPS in HepG2 cells. Cukurova Med J. 2023; 48(1): 268–77.
28. Wang Y, Zhang A, Chen Y, Qi D, Peng C, Liang Z, *et al.* Mechanism of Brucea javanica against multiple myeloma via TNF-NF-κB signaling. Sci Rep. 2025; 15(1): 24311. doi:10.1038/s41598-025-10271-z.
29. Wardhani SP, Nadliroh KA, Aishaqeena AMF, Sonia FA, Suryo Adji AGH, Hanim IM, *et al.* Ganoderma lucidum polysaccharide peptide reduces oxidative stress and improves renal function in patient with cardiometabolic syndrome. Indones Biomed J. 2023; 15(2): 187–93. doi: 10.18585/inabj.v15i2.2137.
30. Ifora I, Abdillah R, Shyntia R. Anti-inflammatory potential of Brucea javanica Fruit. J Drug Delivery Ther. 2022; 12(5-S): 163–7.
31. Thongsepee N, Martviset P, Himakhun W, Chantree P, Sornchuer P, Sangpairoj K, *et al*. Cardiovascular protective effect of Garcinia dulcis flower acetone extract in 2-kidney-1-clip hypertensive rats. Adv Pharmacol Pharm Sci. 2024; 2024: 1–16. doi: 10.1155/2024/9916598.
32. Arthur G, Wasson AR, Straughan RE, Drummond HA, Stec DE. The role of renal medullary bilirubin and biliverdin reductase in angiotensin II-dependent hypertension. Am J Hypertens. 2025; 38(4): 240–7.
33. Ramadhanti R, Helda. Association of hypertension and chronic kidney disease in population aged ≥18 years old. Mol Cell Biomed Sci. 2021; 5(3): 137–44.
34. Chen J, Yu D, Li X, Deng Q, Yang H, Chen L, *et al.* A review of Brucea javanica: Metabolites, pharmacology and clinical application. Front Pharmacol. 2024; 14: 1317620. doi: 10.3389/fphar.2023.1317620.
35. Chaanine AH. Morphological stages of mitochondrial vacuolar degeneration in phenylephrine-stressed cardiac myocytes and in animal models and human heart failure. Medicina. 2019; 55(6): 239. doi: 10.3390/medicina55060239.
36. Li M, Zheng C, Wang H, Wang S. Exploring the antifibrotic mechanisms of ghrelin: Modulating TGF-β signalling in organ fibrosis. Expert Rev Mol Med. 2025; 27: e8. doi: 10.1017/erm.2024.38.
37. Meiliana A, Wijaya A. Resolution to inflammation: Its role in reducing fibrosis and tissue repair. Indones Biomed J. 2023; 15(2): 106–23. doi: 10.18585/inabj.v15i2.2181.
38. Jan-O B, Iampanichakul M, Potue P, Khamseekaew J, Pakdeechote P, Pocasap P, *et al.* Antihypertensive efffects of diosmetin in hypertension-induced cardiovascular abnormalities in rats. J Exp Pharmacol. 2025: 17:667–85.